Global comparison of microwave radiometer, GNSS and ECMWF derived path delays

Joana Fernandes[1], Clara Lázaro[1], Alexandra Nunes[2] and Paolo Cipollini[3]

[1] Universidade do Porto, Faculdade de Ciências; Centro Interdisciplinar de Investigação Marinha e Ambiental – CIIMAR, Portugal
(mjfernan@fc.up.pt)
[2] Instituto Politécnico do Porto, Instituto Superior de Engenharia; CIMAR/CIIMAR-UP, Portugal
[3] National Oceanography Centre, Ocean Observing and Climate, Southampton, UK

Abstract In the scope of the European Space Agency (ESA) funded project COASTALT, a method has been developed to compute the wet tropospheric correction in the coastal regions and applied to Envisat data -- the GNSS-derived path delay (GPD) algorithm (Fernandes et al, 2010). The method has been further refined and applied to the whole Envisat mission in the scope of the ESA Climate Change Initiative (CCI) - Sea Level project.

The GNSS-derived path delays, which play a major role in the GPD algorithm, have to undergo a specific processing, in order to get zenith wet delays (ZWD) at sea level, adequate for merging with valid microwave radiometer (MWR) and ECMWF model derived zenith wet delays. To ensure the consistency of all data types used in the GPD computations, the GNSS-derived path delays have been compared with ECMWF ZWD interpolated at the station locations and with radiometer data at the closest points with valid MWR measurements.

This study presents the details of this comparison, for a global set of 227 GNSS coastal stations, covering the various levels of variability of the tropospheric delay, and MWR data from three missions: Envisat, Jason-1 and Jason-2.

Comparison between GNSS and ECMWF wet path delays (ZWD) From the whole set of coastal GNSS stations used in the GPD computations, a representative set of 227 stations was selected. When more than one station had very close locations, only the station with more observations or the most recent was chosen. For each station and epoch, ECMWF ZWD was first computed at the ECMWF orography level from the global grids of TCWV and 2T (Askne and Nordius (1987) and Mendes (2000)). From the ZWD at ECMWF orography the ZWD at sea level is obtained (Kouba, 2008).

The differences between the GNSS and the interpolated ECMWF ZWD were computed. Table 1 presents the statistical results for seven representative GNSS stations. Fig. 1 and Fig. 2 show the mean difference and the standard deviation, respectively, of the differences (ZWD_GNSS - ZWD_ECMWF) for each station. Fig. 9 to Fig. 15 illustrate the results for some representative stations (labeled in Fig. 1 and Fig. 2).

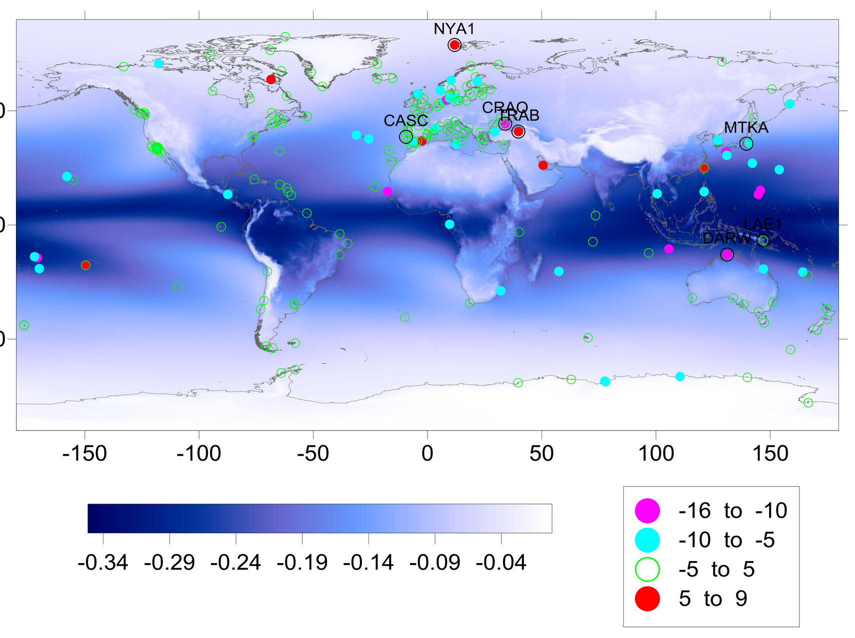

Fig. 1 - Location of the full set of 227 coastal stations with available ZWD solutions. The station colour represents classes of the mean difference between GNSS and ECMW ZWD at each station, in mm. The background colour scale represents the ZWD mean field in meters (from ECMWF).

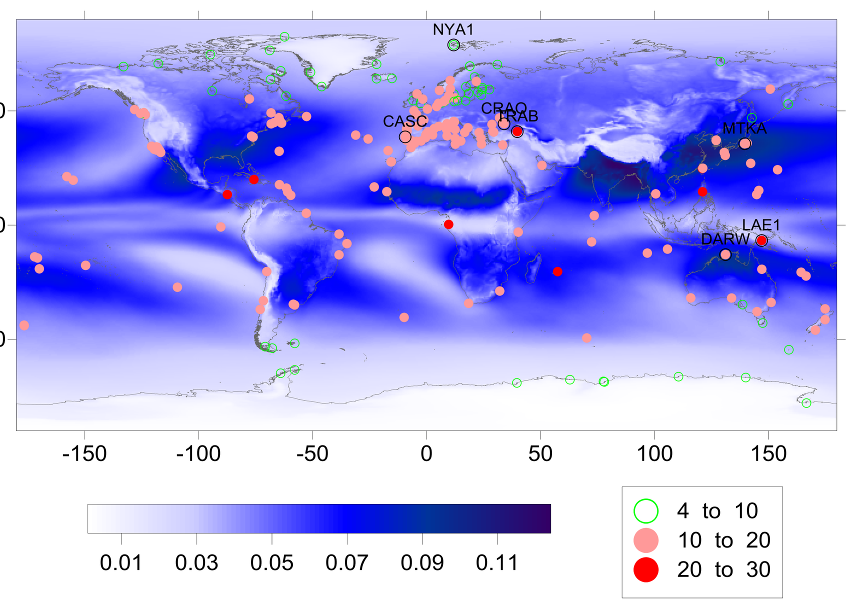

Fig. 2 - Location of the full set of 227 coastal stations with available ZWD solutions. The station colour represents classes of the standard deviation of the differences between GNSS and ECMWF ZWD at each station, in mm. The background colour scale represents the ZWD standard deviation in meters (from ECMWF).

Comparison between GNSS and MWR wet path delays Microwave radiometer (MWR) data, from RADS, were used for Envisat, Jason-1 and Jason-2 for the period [2002-2011] and the cycles referred in Table 2. The time span of each satellite data set is illustrated in Figure 23. Data were stacked, that is, interpolated into reference points along the satellite ground tracks.

For the location and epoch of each altimeter measurement the ZWD from each nearby GNSS station was interpolated for the same epoch. Only satellite points with distances from the coast between 20 and 150 km were considered. Only stations located at distances up to 150 km from each point were analysed.

Only valid MWR data were used. An MWR point is considered invalid whenever one of the following conditions occur: 1) MWR land flag $\neq 0$; 2) MWR interpolation quality flag (for Envisat only) flag $\neq 0$; 3)MWR ice flag $\neq 0$; 4) MWR wet tropospheric correction (WTC) is > 0 m or < -0.5 m; 5) the absolute value of the difference between the MWR and ECMWF WTC is > 10 cm. The first two conditions are mainly related with land contamination near the coast; the last three mainly identify points contaminated by rain or ice.

A statistical analysis was performed for the differences between the interpolated GNSS and the MWR ZWD (ZWD_GNSS-ZWD_MWR). Table 2 presents the global results for all stations and the three satellite missions. Tables 3, 4 and 5 present the results for a set of 7 representative stations and each satellite mission.

Figures 3 to 8 show the mean difference and the standard deviation of the differences for each station and satellite mission. Figures 16 to 22 illustrate the results, for the same stations shown on figures 9 to 15, for the comparison with Envisat MWR. The small number of MWR points available for the comparison with some stations made those comparisons not possible.

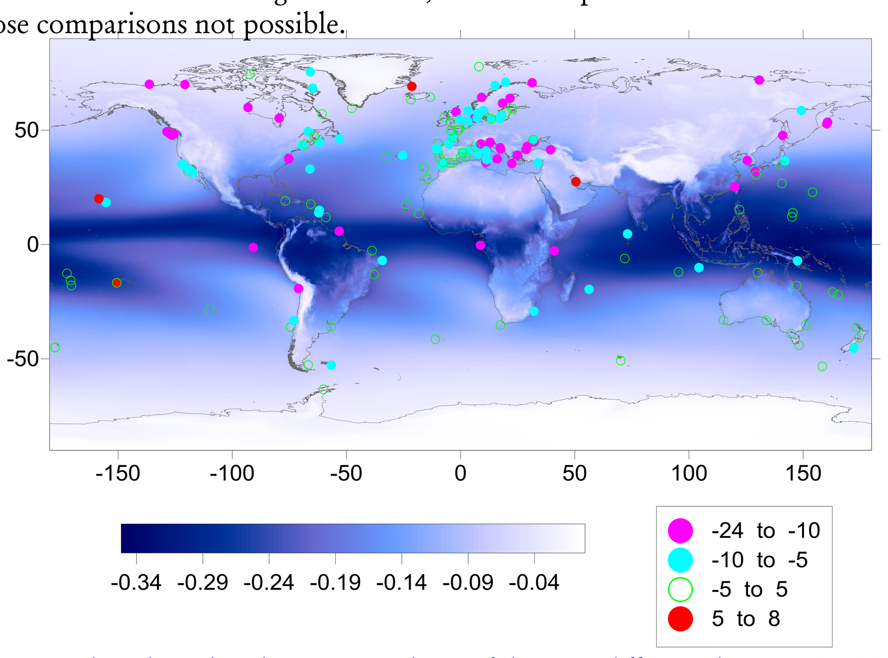

Fig. 3 - The coloured circles represent classes of the mean difference between GNSS and Envisat MWR ZWD at each station, in mm, for a set of 187 stations. The background colour scale represents the ZWD mean field in meters (from ECMWF).

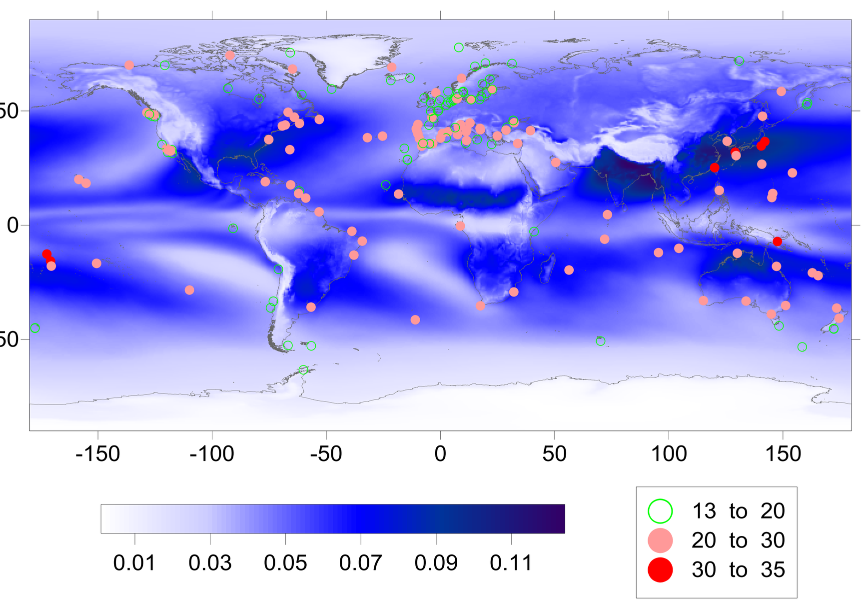

Fig. 4 - The coloured circles represent classes of the standard deviation of the difference between GNSS and Envisat MWR ZWD at each station, in mm, for a set of 187 stations. The background colour scale represents the ZWD standard deviation in meters (from ECMWF).

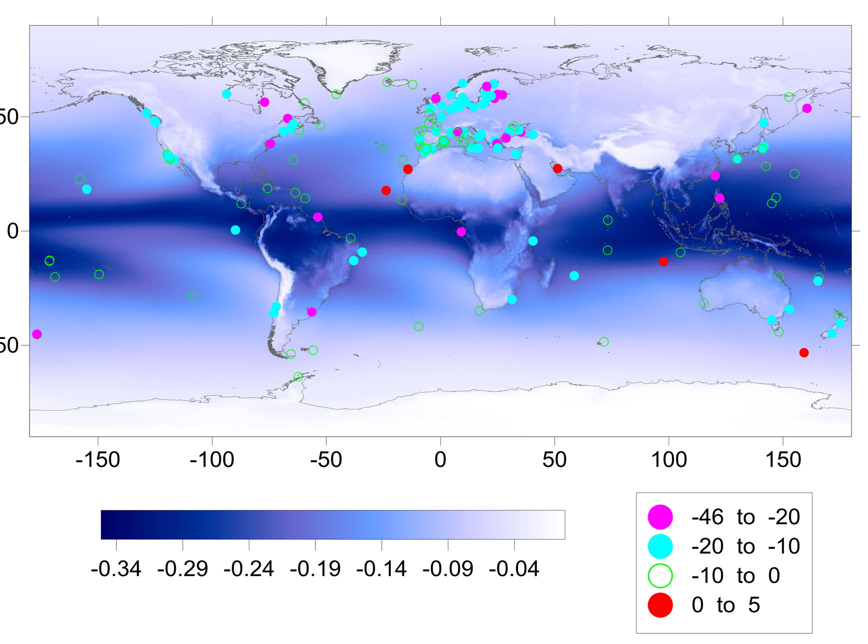

Fig. 5 – Same as on Fig. 3 for Jason-1 and 187 stations.

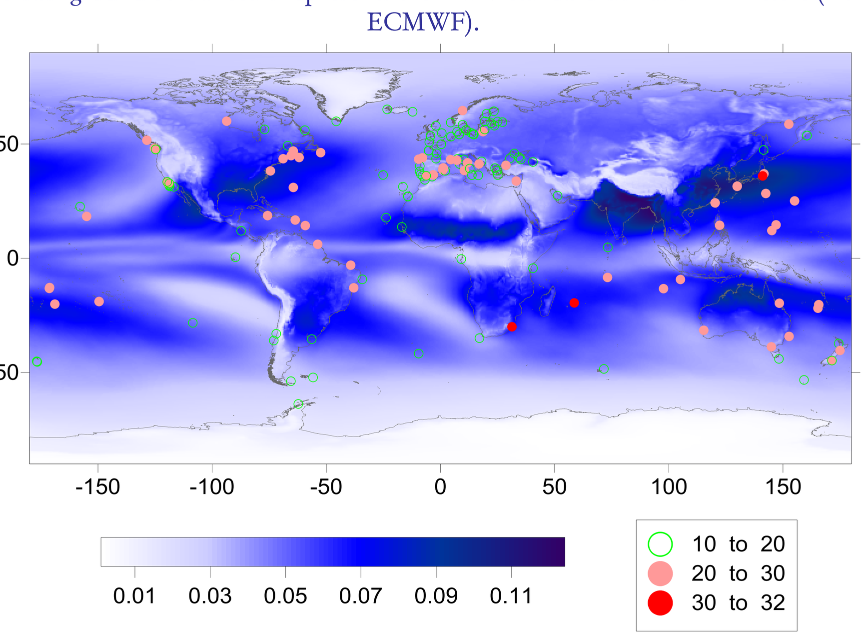

Fig. 6 – Same as on Fig. 4 for Jason-1 and 187 stations.

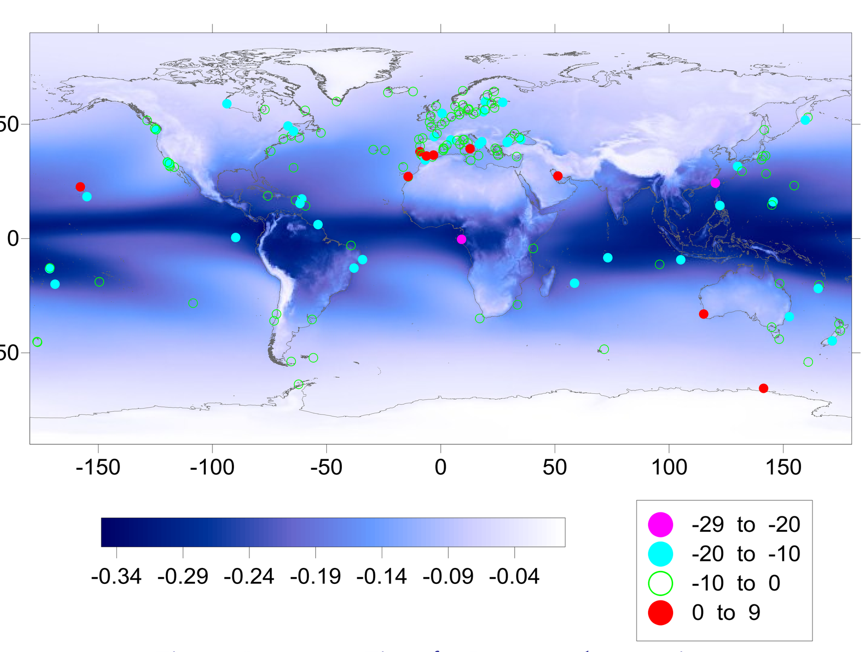

Fig. 7 – Same as on Fig. 3 for Jason-2 and 180 stations.

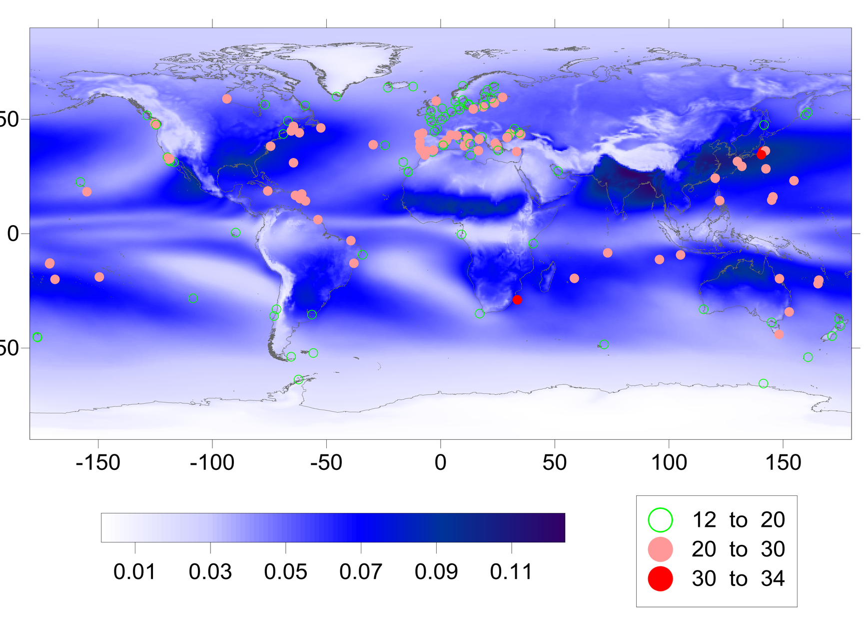

Fig. 8 – Same as on Fig. 4 for Jason-2 and 180 stations.

Table 1 – Statistical results of the differences between GNSS and MWR ZWD, in millimetres, for selected stations.

station	points	mean (mm)	sigma (mm)
CASC	277120	-0.2	12.3
NYA1	290028	0.7	6.0
MTKA	258076	-4.0	14.8
LAE1	86725	1.1	30.1
DARW	238861	-16.4	18.8
CRAO	229574	-15.0	16.6
TRAB	153253	5.5	23.1

Table 3 - Statistical results of the differences between GNSS and Envisat MWR ZWD, in millimetres, for selected stations, for Envisat cycles 10 to 94. Only points up to 150 km from each station and at distances from the coast between 20 km and 150 km were considered.

station	points	mean (mm)	sigma (mm)
CASC	12263	1.2	21.1
NYA1	43380	-4.9	12.6
MTKA	2002	3.1	34.6
LAE1	825	6.6	34.0
DARW	490	-0.5	25.9
CRAO	10960	-23.6	23.0
TRAB	4054	-19.0	22.4

Table 4 - Same as Table 3 for Jason-1 cycles 1 to 262.

station	points	mean (mm)	sigma (mm)
CASC	15619	-2.4	19.9
MTKA	5478	-6.4	30.4
CRAO	6747	-23.4	19.4
TRAB	6130	-18.3	18.3

Table 5 - Same as Table 3 for Jason-2 cycles 1 to 92.

station	points	mean (mm)	sigma (mm)
CASC	5635	4.0	20.2
MTKA	2252	-2.4	30.7
CRAO	2640	-15.8	21.4

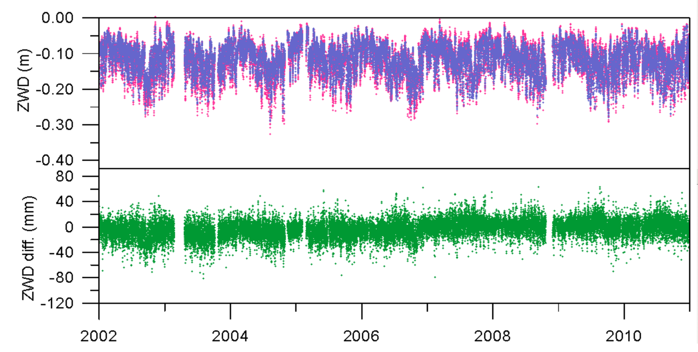

Fig.9 – CASC: comparison GNSS vs. ECMWF

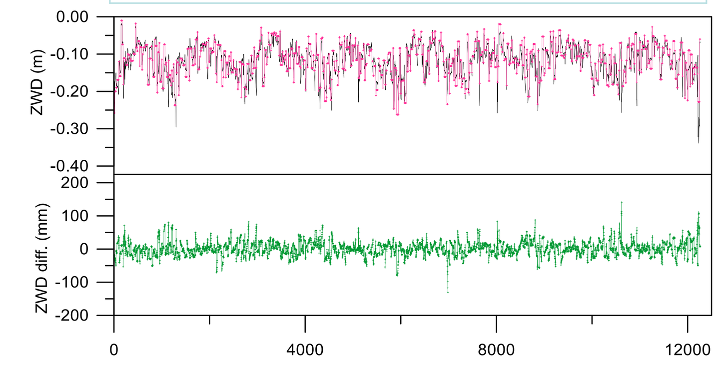

Fig.16 – CASC: comparison GNSS vs. MWR

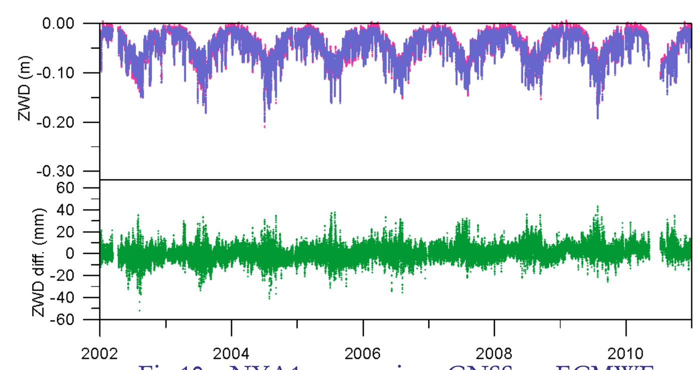

Fig.10 – NYA1: comparison GNSS vs. ECMWF

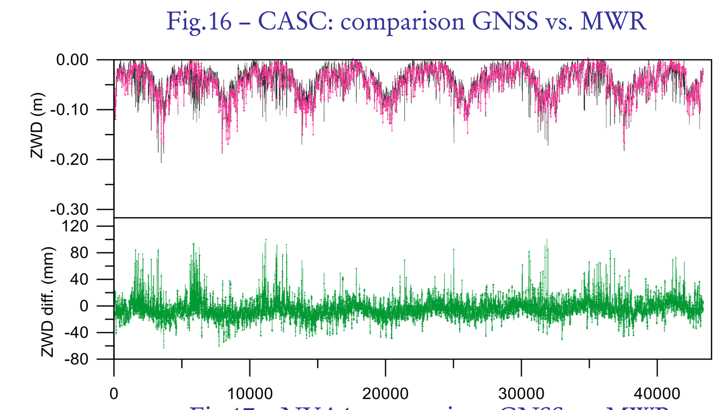

Fig.17 – NYA1: comparison GNSS vs. MWR

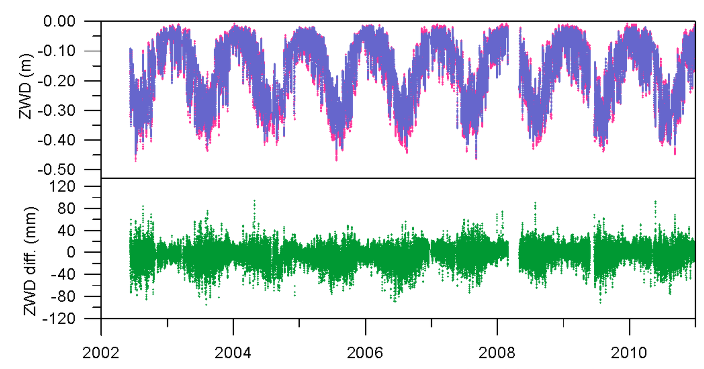

Fig.11 – MTKA: comparison GNSS vs. ECMWF

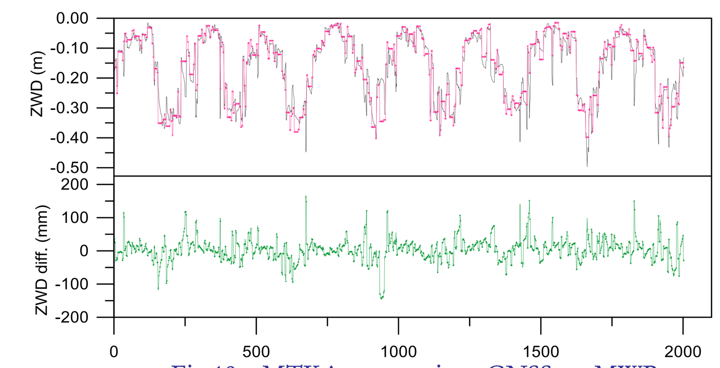

Fig.18 – MTKA: comparison GNSS vs. MWR

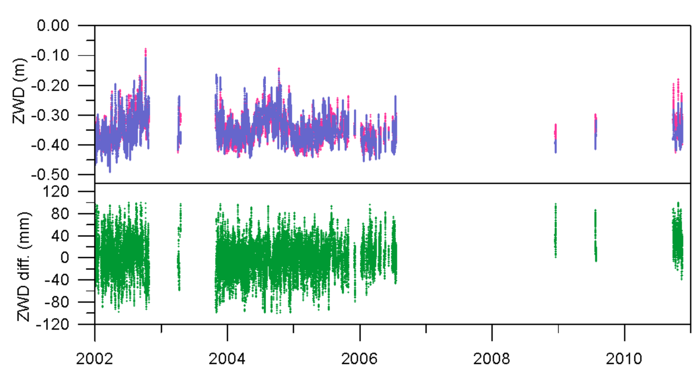

Fig.12 – LAE1: comparison GNSS vs. ECMWF

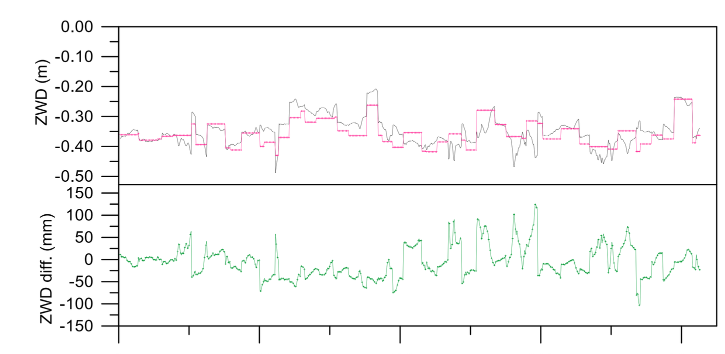

Fig.19 – LAE1: comparison GNSS vs. MWR

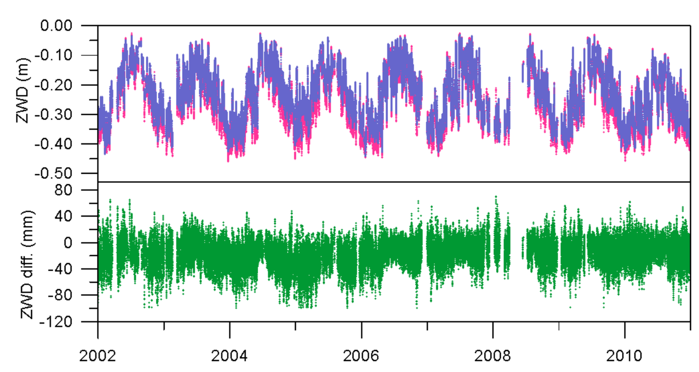

Fig.13 – DARW: comparison GNSS vs. ECMWF

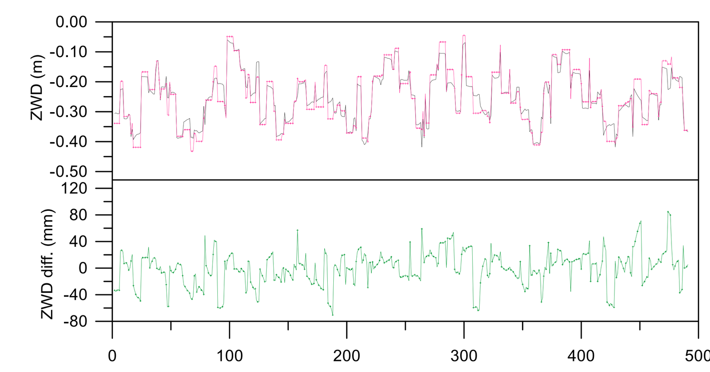

Fig.20 – DARW: comparison GNSS vs. MWR

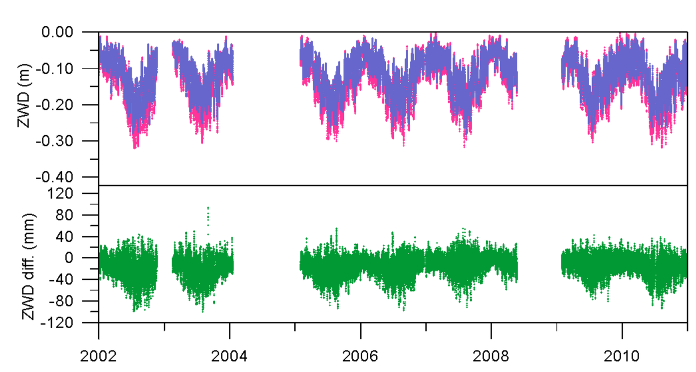

Fig.14 – CRAO: comparison GNSS vs. ECMWF

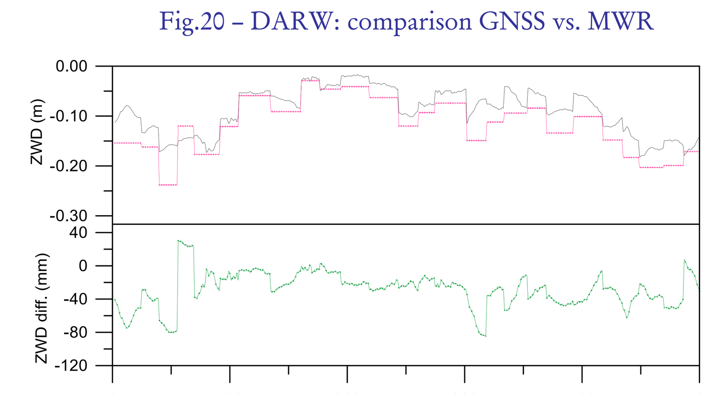

Fig.21 – CRAO: comparison GNSS vs. MWR

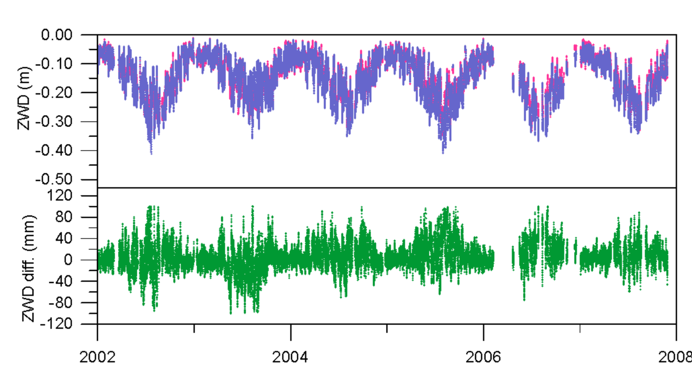

Fig.15 – TRAB: comparison GNSS vs. ECMWF

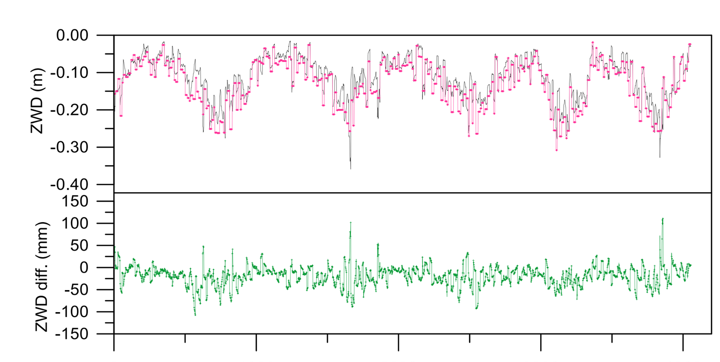

Fig.22 – TRAB: comparison GNSS vs. MWR

Figures 9 to 15 show the GNSS (magenta), the ECMWF ZWD (blue) and the corresponding difference (green) in metres, for the seven stations with labels in Figures 1 and 2. The X axis is time in years.

Figures 16 to 22 show the results, for the same stations, of the comparison between GNSS (magenta) and MWR (black) ZWD at the nearby satellite points in metres. The x axis is point number by ascending time order. Note that consecutive MWR values refer to different points along the satellite track while the GNSS values refer to the ZWD at the station location interpolated to the time of the satellite measurement.

Table 2: Statistics of the differences between GNSS and MWR ZWD, for the various satellite missions, considering all available observations. Only points up to 150km from each station and at distances from the coast between 20 km and 150 km were considered.

satellite	cycles	points	stations	mean (mm)	sigma (mm)
Envisat	10 - 94	1371096	207	-5.6	21.9
Jason-1	1 - 262	1329583	187	-8.7	20.6
Jason-2	1 - 92	631554	180	-6.5	20.3

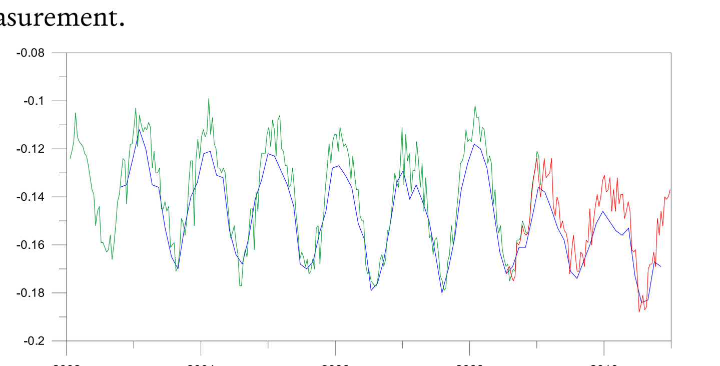

Fig.23 (on the right) – Mean value of the ZWD field for each satellite cycle: Envisat (blue), Jason-1 (green) and Jason-2 (red).

Discussion Overall there is a very good agreement between the ZWD derived from the GNSS path delays (ZWD_GNSS) and the corresponding value determined from ECMWF (ZWD_ECMWF). Considering the whole set of 227 stations, the mean difference between these fields is -3 mm and has values between -16 mm and 9 mm. The standard deviation of the differences for the 227 stations is 13 mm and ranges between 4 mm and 30 mm. Eight stations have standard deviations larger than 20 mm. The global comparison between the ZWD from GNSS (ZWD_GNSS) and from MWR (ZWD_MWR) shows a mean value between -6 mm and -9 mm for the 3 missions. Considering the individual stations the mean ranges between -46 mm and 5 mm. The standard deviation has values between 20 mm and 22 mm for the 3 missions. Considering the individual stations the standard deviation ranges between 10 and35 mm. Since these differences represent the spatial variability of the WTC in the oceanic coastal region around a GNSS station, with a radius of 150 km, these are within the expected range. Note that the period of the analysis for each satellite is not the same and therefore the values for the three missions are not directly comparable. Figures 9 to 23 show examples of seven representative stations whose location is shown in Figures 1 and 2. CASC is an example of a station with typical statistical values for both the comparison with ECMWF and MWR. NYA1 is an example of a station at high latitude, with a small standard deviation of the ZWD field and therefore of the analysed differences.

MTKA is an example of a station with a relatively low value of the standard deviation of the differences between GNSS and ECMWF ZWD (15 mm) but with large values for the equivalent comparison between GNSS and MWR ZWD (30-36 mm). LAE1 is an example of a station with a large standard deviation of the difference for all comparisons. This seems to be an unstable station with large data gaps. DARW shows a bias of -16 mm wrt to ECMWF but no significant bias wrt Envisat MWR. CRAO shows a relatively large bias both wrt ECMWF (-15 mm) and Envisat MWR (-24 mm). TRAB is an example of a station with a small but positive bias wrt to ECMWF (6 mm) but a relatively large negative bias wrt both Envisat and Jason-1 (~-19 mm). This shows that it is very difficult to ascertain the computed differences to biases of a given data set.

For some stations such as MTKA, LAE1,and TRAB, some radiometer points still exist with relatively extreme values, most probably due to rain or ice contamination. Overall, we can conclude that no significant biases or trends were found between the three analysed data sets and that the procedure adopted to process the GNSS-derived ZWD seems appropriate. During this study it became evident that noisy MWR measurements still persist after data screening using the available land and rain/ice radiometer flags,

The results show that the rejection criteria applied to the MWR measurements revealed to be rather efficient in removing the majority of noisy MWR points which otherwise would appear as outliers in the comparison with GNSS data. This highlights the importance of identifying and removing the noisy MWR values, which otherwise, in the estimation process implemented in the GPD algorithm, would contaminate the estimation of a valid wet tropospheric correction in the surrounding points.

References

Askne J and Nordius H (1987), Estimation of tropospheric delay for microwaves from surface weather data, Radio Sci., 22(3), 379–386, doi:10.1029/RS022i003p00379
Fernandes J, Lázaro C, Nunes A, Pires N, Bastos L and Mendes V (2010), GNSS-Derived Path Delay: an approach to compute the wet tropospheric correction for coastal altimetry. IEEE Geosci Remote Sens, 7(3), 596-600. doi:10.1109/LGRS.2010.2042425
Kouba J (2008), Implementations and testing of the gridded Vienna Mapping Function 1(VMF1), J Geod, 82, 193-205. doi:10.1007/s00190-007-0170-0
Mendes VB, Prates G, Santos L, Langley RB (2000), An evaluation of the accuracy of models of the determination of the weighted mean temperature of the atmosphere. Proceedings of ION 2000 National Technical Meeting, January 26-28, Anaheim, CA.

Acknowledgements

This work has been performed in the scope of project COASTALT (*ESA AO/1-5429/07/I-LG*) and project CALITRO (approved within the OSTST 2007 research announcement). Altimeter data used in this study include Envisat GDRs and RADS data. A grateful thanks to Remko Scharroo (NOAA/Altimetrics LLC) for his invaluable help on dealing with RADS data. The authors would like to acknowledge the European Centre for Medium Range Weather Forecasts (ECMWF) for providing the reanalysis data on the single-level atmospheric fields of the Deterministic Atmospheric Model.